Journal of Visualized Experiments

Morphology-based distinction between healthy and pathological cells utilizing Fourier transforms and Self-Organizing Maps

--Manuscript Draft--

Article Type:	Invited Methods Article - JoVE Produced Video
Manuscript Number:	JoVE58543R1
Full Title:	Morphology-based distinction between healthy and pathological cells utilizing Fourier transforms and Self-Organizing Maps
Keywords:	Shape analysis Fourier transform Imaging 2-photon microscopy Immunology Artificial intelligence Self-Organizing Maps
Corresponding Author:	Zoltan Cseresnyes Leibniz-Institut fur Naturstoff-Forschung und Infektionsbiologie eV Hans-Knoll-Institut Jena, GERMANY
Corresponding Author's Institution:	Leibniz-Institut fur Naturstoff-Forschung und Infektionsbiologie eV Hans-Knoll-Institut
Corresponding Author E-Mail:	Zoltan.Cseresnyes@hki-jena.de
Order of Authors:	Fabian L. Kriegel
	Ralf Köhler
	Jannike Bayat-Sarmadi
	Simon Bayerl
	Anja E. Hauser
	Raluca Niesner
	Andreas Luch
	Zoltan Cseresnyes
Additional Information:	
Question	**Response**
Please indicate whether this article will be Standard Access or Open Access.	Open Access (US$4,200)
Please indicate the **city, state/province, and country** where this article will be **filmed**. Please do not use abbreviations.	Department of Chemical and Product Safety, German Federal Institute for Risk Assessment (BfR), Max-Dohrn-Strasse 8-10., Berlin 10589, Germany

Powered by Editorial Manager® and ProduXion Manager® from Aries Systems Corporation

Editorial Board
Journal of Visualized Experiments

Dr. Zoltan Cseresnyes
Hans Knöll Institute Jena
Applied Systems Biology
Beutenbergstr. 11a
07745 Jena, Germany
Phone +49 (0)3641-5321532
zoltan.cseresnyes@hki-jena.de

Jena, 6th of July, 2018

Dear Dr. Nam Nguyen,

We would like to thank you and the reviewers for the thorough and extremely useful review of our manuscript entitled
"Morphology-based distinction between healthy and pathological cells utilizing Fourier transforms and Self-Organizing Maps " by Kriegel et al.
Hereby we are submitting the revised version to be considered for publication in the Journal of Visualized Experiments.

We have answered all questions and comments by both the Editor and the Reviewers according to our best ability. These are provided in a separate document.

The main text has been edited according to these changes; all new and edited parts are highlighted in purple, in order to make finding the parts in question easier.

We updated our auto-rotation Python script so that it now provides a GUI, as requested by Reviewer 2. We also updated the two associated videos according to this change (including one that was erroneously recorded from a blank screen).

Some of these data have been reported before (Kriegel, F. L. *et al.* Cell shape characterization and classification with discrete Fourier transforms and self-organizing maps. *Cytometry Part A.* **93** (3), 323-333, doi:10.1002/cyto.a.23279 (2018)). For the material that we re-used from this publication (Figures 2-5) we have received copyright permission from the publisher John Wiley and Sons and we upload this as pdf. We declare no conflict of interest. All authors concur with the submission and hope that you will find our manuscript appropriate for publication in your journal.

With best regards,

Zoltan Cseresnyes

Manuscript Click here to download Manuscript 58543_R1.docx

TITLE:

Morphology-Based Distinction between Healthy and Pathological Cells Utilizing Fourier Transforms and Self-Organizing Maps

AUTHORS AND AFFILIATIONS:

Fabian L. Kriegel[1,2], Ralf Köhler[2], Jannike Bayat-Sarmadi[2], Simon Bayerl[3], Anja E. Hauser[2,3], Raluca Niesner[2], Andreas Luch[1,*], Zoltan Cseresnyes[4,2 *]

[1] Department of Chemical and Product Safety, German Federal Institute for Risk Assessment (BfR), Berlin, Germany
[2] Deutsches Rheuma-Forschungszentrum (DRFZ) Berlin, a Leibniz Institute, Berlin, Germany
[3] Charité Universitätsmedizin Berlin, Berlin, Germany
[4] Applied Systems Biology, Leibniz Institute for Natural Product Research and Infection Biology Hans Knöll Institute, Jena, Germany

*shared senior authors

Fabian.Kriegel@bfr.bund.de
Ralf.Koehler@drfz.de
sarmadi@drfz.de
simon.bayerl@charite.de
hauser@drfz.de
niesner@drfz.de
andreas.luch@bfr.bund.de
Zoltan.Cseresnyes@hki-jena.de

Correspondence to:
Andreas Luch
Zoltan Cseresnyes

KEYWORDS:

shape analysis; Fourier transform; imaging; 2-photon microscopy; immunology; artificial intelligence; Self-Organizing Maps

SUMMARY:

Here, we provide a workflow that allows the identification of healthy and pathological cells based on their 3-dimensional shape. We describe the process of using 2D projection outlines based on the 3D surfaces to train a Self-Organizing Map that will provide objective clustering of the investigated cell populations.

ABSTRACT:

The appearance and the movements of immune cells are driven by their environment. As a reaction to a pathogen invasion, the immune cells are recruited to the site of inflammation and are activated to prevent a further spreading of the invasion. This is also reflected by changes in

the behavior and the morphological appearance of the immune cells. In cancerous tissue, similar morphokinetic changes have been observed in the behavior of microglial cells: intra-tumoral microglia have less complex 3-dimensional shapes, having less-branched cellular processes, and move more rapidly than those in healthy tissue. The examination of such morphokinetic properties requires complex 3D microscopy techniques, which can be extremely challenging when executed longitudinally. Therefore, the recording of a static 3D shape of a cell is much simpler, because this does not require intravital measurements and can be performed on excised tissue as well. However, it is essential to possess analysis tools that allow the fast and precise description of the 3D shapes and allows the diagnostic classification of healthy and pathogenic tissue samples based solely on static, shape-related information. Here, we present a toolkit that analyzes the discrete Fourier components of the outline of a set of 2D projections of the 3D cell surfaces *via* Self-Organizing Maps. The application of artificial intelligence methods allows our framework to learn about various cell shapes as it is applied to more and more tissue samples, whilst the workflow remains simple.

INTRODUCTION:

Timely, simple and precise determination of the pathological status of biological tissue is of the highest interest in biomedical research. Mouse models provide the means to study a range of pathological conditions, such as immune reactions or cancer development, in combination with complex 3D and 4D (3 spatial dimensions and time) microscopy techniques. Microscopy studies can be performed *via* intravital or excised-tissue 2-photon microscopy, light-sheet microscopy, and -to a limited tissue depth of approximately 100 µm- by confocal microscopy. In order to have time-related information about the cells' behavior under physiological or pathological conditions, it is necessary to monitor the tissue for an extended period of time, which usually requires intravital imaging[1,2]. Naturally, the applicability of this technique is limited to animal models due to its invasiveness. Non-invasive techniques are also available for human applications, including a variety of tomography methods (MSOT, CT, *etc.*), but these methods all lack the necessary spatial –and often temporal- resolution to study behavior at the cellular level.

Static information regarding the appearance of cells may be accessible more easily *via* various 3D imaging techniques executed on excised tissue samples. Here, the kinetic behavior of the cells is not measured, thus it is necessary to adopt novel analysis techniques that are able to determine the pathogenic status of the examined cells based solely on their morphology[3]. Such an approach was used to link cell shapes and tissue textures to pathological behavior[4-6].

In the new technique described here, the cells are reconstructed as 3D surfaces and their shapes are characterized *via* 3D-to-2D projections and successive Fourier-based periphery-shape analysis[7,8]. By reducing the dimensions from 3 to 2, the problem is simplified. It is also possible to characterize the cell surfaces in 3D by applying spherical harmonics analysis, as it has been done for medical images[9]. However, spherical harmonics do not handle sharp and rugged shapes well, requiring a multi-scale grid to be established on the unit sphere. In addition, the number of necessary spherical harmonics components can be large (50-70), with the underlying calculations very demanding and the results hard to interpret[10-12].

With our newly proposed method, the task is reduced to a series of 2D shape descriptions, where the number of the 2D projections is up to the analyst and can be adjusted according to the complexity of the 3D shape. The projections are generated automatically *via* a Python script that runs inside a 3D animation tool. The 2D projections are described by the discrete Fourier transform (DFT) components of their periphery, calculated by a Fiji[13] plugin that is provided here as part of our software package. The DFT is applied here in order to decompose the complex outline of the cell into a series of sin and cos functions. In this way, we can describe the outline with a relatively small number of DFT components, thus reducing the complexity of the problem (for further details see Equations section). The DFT components are put into a trained Self-Organizing Map (SOM[14]), where the existence of shape clusters can be objectively tested[8]. SOMs provide a competitive and unsupervised learning tool from the field of artificial intelligence. They consist of a linked array of artificial neurons which communicate with each other *via* a weighted neighborhood distance function. The neuronal system responds to the first element of the input dataset and the neurons whose response is the strongest are "grouped" nearer to each other. As the neural system receives more and more input, data neurons that repeatedly respond strongly start to form well defined cluster within the system. After proper training on a large dataset that contains 2D shape information in form of a set of DFT components, any individual cell's DFT components can be put into the trained SOM and reveal whether the cell likely belongs to the healthy or the pathogenic cell group. We expect such tool to become a great addition to the methods of scientific and clinical diagnostics.

PROTOCOL:

1. Protocol Requirements

1.1. Obtain high-resolution deconvolved three-dimensional (3D) microscopy data deconvolved in compliance with the Nyquist criterion with a sampling interval at least twice the highest spatial frequency of the specimen to obtain a high resolution image.

1.2. Use 3D rendering software for the surface reconstruction and export.

1.3. Use 3D animation software capable of running Python scripts (the Python script can be downloaded from the github repository: https://github.com/zcseresn/ShapeAnalysis) to create 2D projections.

1.4. Use Fiji[13] to analyze 2D projections and extract the DFT components.

1.4.1. Use the current Fiji distribution. If there already exists an installed version of Fiji, make sure that the installed version is the latest. This can be easily achieved by running the **Help |Update** option.

1.4.2. Use the Active Contour plugin[15], which can be downloaded from http://imagejdocu.tudor.lu/doku.php?id=plugin:segmentation:active_contour:start and should be copied into the plugins folder.

1.4.3. Download the SHADE Fiji plugin from the github repository and copy into the plugins folder.

1.5. Use computational mathematics software capable of calculating Self-Organizing Maps.

2. Reconstruct the 3D Image.

Note: For testing purposes, an example dataset is provided in the github repository (see above).

2.1. Start the 3D reconstruction software and open the 3D image data.

2.2. Create a 3D Surface of (all) object(s).

2.2.1. Select the **3D view** option and click on **Surfaces**. Click on the **Next** button (blue circle with a white triangle) to proceed with the surface creation wizard.

2.2.2. Select the image channel for the surface reconstruction.

2.2.3. Apply a smoothing function to avoid porous surfaces.

2.2.3.1. Choose a smoothing value that does not hide the details of the surface but avoids porous surfaces.

2.2.4. Select a thresholding method to find the surfaces.

2.2.4.1. Use an absolute intensity threshold when the objects are well-separated from the background and have an approximately uniform brightness level.

2.2.4.2. Apply a local contrast threshold when the objects vary in their intensity but can still be separated from the local background and from the other objects surrounding them. Set the local threshold search area according to the value of the expected diameter of the reconstructed objects.

2.2.5. Filter the reconstructed surfaces according to morphological parameters of interest, *e.g.,* volume, sphericity, surface-to-volume ratio, *etc.*, and finish the surface reconstruction.

2.3. Save and export the generated surfaces in a format that is compatible with the 3D animation software that will be used in the next step.

3. Transform the 3D reconstructed surfaces into 2D projections

3.1. Start Blender and go to the output tab in the right-side window. Select the TIFF format from the dropdown menu and set the color depth to 8 bit RGBA.

2.2. Switch into Scripting Mode and open the provided script file "GUI_AutoRotate.py" from the repository provided with this work (https://github.com/zcseresn/ShapeAnalysis).

2.3. Click on **Run Script**. Choose the folder of the wrl files when prompted for input.

2.4. If needed, create more rotations when working with more complex surfaces: go to the **GUI** and set the box **Rotations** to a value above 6.

Note: A rotation of 6 different angles can be sufficient to distinguish the different cell populations. It is not recommended to create less than six rotations per surface, because of potential information loss.

2.5. Run the script by clicking on the **Rotate** button in the GUI. Save the projections of the individual surfaces in the same folder that was used as the input folder (step 2.3). By default, the images are saved in an 8 bit Tiff format (see step 2.1), which is the format required by the Fiji plugin SHADE.

4. Find the periphery and calculate the Fourier components using Fiji.

4.1. Open Fiji and select **SHADE** in the Plugins menu. Start with the default values and fine-tune the parameters later on. Click **OK** when ready to run the program.

4.1.1. Choose a **Gradient Threshold** value for the thresholding of the input image.

4.1.2. Choose the **Number of Iterations**. The higher the **Number of Iterations** value, the more precise the reconstruction of the periphery. For simpler shapes, a lower number is usually sufficient.

4.1.3. Use the **Number of Dilations** parameter to determine how much larger the starting mask is compared to the actual cell. Usually more complex shapes need more dilation steps for proper periphery finding.

4.1.4. Check the **Dark Background** checkbox if the projected shapes are brighter than the background.

4.1.5. Activate the **Show Intermediate Results** checkbox only when using a small test dataset to determine the performance of SHADE. Activating this option for larger datasets lowers the computational efficiency and could possibly halt a system with low video memory.

4.1.6. Check the **Save Result Tables** checkbox to use the results of SHADE as an input for step 5. If the box is checked, all results are saved in individual csv files. A summary of the output data is always generated in a file called "Result_collection_of_all_DFT_calculations.csv".

4.2. Select the input data folder that contains the TIFF files that were created in step 3.

4.3. Provide the output data folder.

4.4. Click **OK** to start the plugin.

5. Self-Organizing Maps

Note: SOM networks are only able to classify data when they are trained on a large dataset which contains input from all expected cell types and conditions. For demonstration purposes, such a dataset is provided and can be found in our repository ("AllCells_summary_normalised.csv" from https://github.com/zcseresn/ShapeAnalysis

5.1. Follow these guidelines if there is no trained SOM available yet for the input data; otherwise proceed to step 5.2.

5.1.1. Start a computational mathematical software capable of performing neural network classifications.

5.1.2. Select a data file to be used for training the SOM network. This dataset should contain all experimental conditions in order to train the SOM on the particular cell types and experimental conditions.

Note: It is also possible to use the provided AllCells_summary_normalised.csv for testing the system.

5.1.3. Start the training and wait till the training is completed before proceeding. By default, the script is set to run 2000 iterations ("Epochs").

Note: The number of iterations depends on the learning rate of the SOM. Depending on the input data it is advisable to test both higher and lower number of epochs and observe the stability of the pattern of the SOM. When using the script provided, the number of iterations can be changed under line 32. The network size can be changed in line 34 (by default it is set to 12 by 12).

5.1.4. After the training is finished, examine the network's topology (neighbor distances, input planes, sample hits, *etc.*). The network is now trained and can be saved for future use.

5.2. Load in the SOM, when using an already trained map (this can come either from Step 5.1 or from other sources) in order to cluster a dataset.

5.2.1. Import the csv file that is to be tested with the preloaded trained SOM. Select the csv output of the SHADE Plugin from step 4 when using data prepared by the SHADE plugin.

Note: It is also possible to use the example data files "InteractingCells_summary_normalised.csv", "MobileCells_summary_normalised.csv" or "PhagocytosingCells_summary_normalised.csv" that are provided *via* github.

5.2.2. After the classification is finished, evaluate the results of the SOM as in step 5.1.5.

5.2.2.1. Examine the hitmap generated from the csv file. Each cell of the map shows how many times the dataset "hits" that particular cell of the trained SOM. When a group of cells are clustered in a small area of this map, this indicates that the dataset is fairly homogenous. Multiple clusters will indicate that subgroups likely exist in the dataset.

5.2.2.2. Examine the neighborhood weight distances. Areas of this map that are well separated correspond to groups of objects that behave very differently from the SOM's point of view. With DFT components as input data, this means that these cell groups have very dissimilar shapes of the corresponding 3D surfaces.

5.2.2.3. Examine the weight planes for information about the contribution by each element of the feature vector. In case of using the 20 DFT components as described earlier, 19 maps will appear here. When using the provided example dataset, the first 5 or 6 weight planes will be different, but the rest of them will appear fairly similar. In this case it can be concluded that it would be enough to use approximately 7 DFT components.

REPRESENTATIVE RESULTS:

We applied a DFT to calculate the main components of the shape corresponding to the cell projections. The Fourier descriptors were obtained by applying the DFT algorithm to the xy-coordinate pairs of the fitted periphery of the cell projections, obtained as the output of the AbSnake part of our workflow. These xy-coordinate pairs can be handled as a complex-valued 2D vector "g":

$$g = (g_0, g_1, \dots, g_{N-1})$$

From the vector "g", we use DFT to calculate the complex-valued Fourier spectrum:

$$G = (G_0, G_1, \dots, G_{N-1})$$

Based on well-known formulas of the discrete Fourier spectrum, and using the complex-number labeling of "g" as:

$$G_k = R_k + I \cdot I_k$$

We get:

$$R_k = \frac{1}{N} \cdot \sum_{n=0}^{N-1} [R_n + I \cdot I_n] \cdot \left[\cos\left(R_n \frac{n}{N}\right) - I \cdot \sin\left(R_n \frac{n}{N}\right)\right] \quad (1)$$

We can calculate the real ("A") and imaginary ("B") components of $\square_{\square} = (\square_{\square} + \square \cdot \square_{\square})$:

$$\square_{\square} = \square\square(\square_{\square}) = \frac{1}{\square}\sum_{\square=0}^{\square-1}\left[\square_{\square} \cdot \cos\left(\square_{\square}\frac{\square}{\square}\right) + \square_{\square} \cdot \sin\left(\square_{\square}\frac{\square}{\square}\right)\right] \quad (2)$$

$$\square_{\square} = \square\square(\square_{\square}) = \frac{1}{\square}\sum_{\square=0}^{\square-1}\left[\square_{\square} \cdot \cos\left(\square_{\square}\frac{\square}{\square}\right) - \square_{\square} \cdot \sin\left(\square_{\square}\frac{\square}{\square}\right)\right] \quad (3)$$

Here, the first DFT component G_0 corresponds to m = 0, which gives:

$$\square_0 = \frac{1}{\square}\sum_{\square=0}^{\square-1}[\square_{\square} \cdot \cos(0) + \square_{\square} \cdot \sin(0)] = \bar{\square} \quad (4)$$

$$\square_0 = \frac{1}{\square}\sum_{\square=0}^{\square-1}[\square_{\square} \cdot \cos(0) - \square_{\square} \cdot \sin(0)] = \bar{\square} \quad (5)$$

Consequently, this component describes the geometrical center of the original object.
The second element of the DFT forward spectrum, G_1, corresponds to m = 1:

$$\square_{\square}^{(1)} = \square_1 \cdot \square^{\square 2\square\frac{\square}{\square}} = (\square_1 + \square \cdot \square_1) \cdot \left(\cos\left(2\square\square\frac{\square}{\square}\right) + \square \cdot \square\square\left(2\square\square\frac{\square}{\square}\right)\right) \quad (6)$$

From Eq.6 we conclude that these points form a circle with a radius of $\square_1 = |\square_1|$ and starting angle $\square = \square\square\square^{-1}\left(\frac{\square_1}{\square_1}\right)$, where the circle describes one complete revolution while the shape is traced once. The center of the circle is located at the origin (0, 0), the radius is $|G_1|$ and the starting point is:

$$\square_0^{(1)} = \square_1 \cdot \square^{\square 2\square\square\frac{\square}{\square}} = \square_1 \cdot \square^{\square 2\square 1\frac{0}{\square}} = \square_1 \cdot \square^0 = \square_1 \quad (7)$$

In general, for a single Fourier coefficient $\square_{\square} = (\square_{\square}, \square_{\square})$, the coordinates are described as:

$$\square_{\square}^{(\square)} = \square_{\square} \cdot \square^{\square 2\square\square\frac{\square}{\square}} = [\square_{\square} + \square \cdot \square_{\square}] \cdot \left[\cos\left(2\square\square\frac{\square}{\square}\right) + \square * \sin\left(2\square\square\frac{\square}{\square}\right)\right] \quad (8)$$

Similarly to Eq.6, Eq.8 also describes a circle, but with a radius of $R_m=|G_m|$, a starting angle $\square\square\square^{-1}\left(\frac{\square_{\square}}{\square_{\square}}\right)$ and a starting point at $\square_0^{(\square)} = \square_{\square}$, where the contour is traced once whilst the circle runs through "m" full orbits [16,17].

Shape parameters as SOM input

The workflow, as described in **Figure 1**, was applied to a deconvolved (using a measured Point Spread Function) intravital multi-photon microscopy dataset of microglial cells to characterize

their morphological changes in healthy or cancerous cortical tissue[18]. Twenty DFT components were calculated for each 2D projection of the reconstructed 3D surfaces and the results were used as an input for the SOM training. Under physiological conditions, the microglia presented a rather complex shape with multiple, highly branched processes (**Figure 2a**). When placed in a cancerous environment (cortical tumor model), the microglia changed to a simpler, more spindle-like shape (**Figure 2b**).

The trained SOM was tested in order to evaluate its ability to distinguish between healthy and cancerous cells. The healthy cell population was projected onto a single area of the SOM (**Figure 2c**). The SOM responded to the cancerous microglia dataset with a dumbbell-shaped active region (**Figure 2d**). A blindly mixed input data set that consisted of DFT shape components from both the healthy and the cancerous group was projected by the SOM into two distinct groups, whilst keeping the shape of their individual contours similar to those of the separated groups (**Figure 2e**; compare with **2c** and **2d**). It can be concluded that the mixed dataset was successfully clustered by the SOM.

We tested the performance of the SOM by comparing its projections with the manual analysis of the same data by a medical expert, who classified the dataset based on their spatio-temporal behavior. The expert identified four distinct cell groups (resting cells, phagocytosing cells, interacting cells, and mobile cells [18]), which were reconstructed and used to train a 12x12 SOM. The trained network (**Figure 3a**) shows groups of high hit-value artificial neurons, especially in the bottom left and the middle areas of the SOM. The response of the trained network was also tested with four randomly selected subsets (which were not part of the training dataset) of images from the four different groups identified by the expert[18]. These image subsets resulted in four well-defined responses by the SOM, as shown in **Figure 3b**. The resting cells exhibit the most complex shape and showed the highest separation level within the neural network (**Figure 3b** "resting" panel). The other three identified cell types shared a common area of the SOM in the bottom left corner, but were otherwise separated by the SOM. The bottom left corner SOM area thus corresponds to the lower-index DFT values.

The robustness of the SOM approach was tested by using the trained SOM with three random subsets of the same -resting- cell type (not part of the training dataset). The response of the SOM to this input exhibits a very similar response (**Figure 3c**, subsets 1-3), demonstrating the robustness of our approach.

Time-dependent cell shape changes are precisely characterized by DFT

In order to examine the effect of time-dependent changes of the cell shape on the DFT components, one to three cells per subgroup (see **Figure 3b**) were tracked for 13 to 28 time points. **Figure 4** shows the first ten DFT components of a mobile cell (**Figure 4a**) and an interacting cell (**Figure 4b**), which were plotted as a function of time. The mobile cell exhibits a permanently altering shape (see Supplementary Video 4 in [8]), which is reflected by a rougher DFT surface. The bursts of the DFT amplitude in the first third of the time course for the interacting cell coincide with the fast and vast cell shape changes as shown in Supplementary Video 5 in [8].

The time course of all 19 DFT components was also characterized for these two cells at three separate time points during the tracking of a mobile cell (**Figure 5a**) and of an interacting cell (**Figure 5b**). The perpendicular axes represent hereby the six rotation angles and indicate that all projections are equally important for the characterization of the shape for both cell types.

FIGURE LEGENDS

Figure 1. Step by step workflow of the data processing to identify cell clustering based on the shape of cells. Surfaces reconstructed in 3D were used as input to Blender for automated 3D-to-2D projections. The periphery of each projection was located and the DFT components were calculated. The components served as an input either to a trained SOM in Matlab, or to train a new SOM.

Figure 2. Typical appearance of mouse cortical microglia cells under control conditions (a) and in cancerous tissue (b) Screenshots of reconstructed microglia surfaces. SOM projections were created from the three groups of microglia samples from the mouse cortex: control (non-tumorous) cells (c), tumor cells (d), and a mixed population of cells (e). This figure has been modified with permission[8].

Figure 3. (a, left) Self-Organizing Map of a mouse microglia dataset consisting of 768 input feature vectors. The dataset was used to train a 12x12 artificial neural network, using hexagonal neighborhood geometry, random initialization and 2000 epochs. (a, right) The corresponding SOM input planes of the first 10 DFT components (b) The responses of the SOM depicted in (a), to one random VRML file subset each from the four cell types "mobile," "interacting," "resting," and "phagocytic" as first described in Figure 5 of Bayerl *et al.*[18]. (c) The response of the same SOM as in (a, left) to three random subsets of the entire dataset (which were thus not part of the training dataset) of the "resting cells"-type 3D surfaces. The similarity amongst the three responses is notable. This figure has been modified with permission[8].

Figure 4. (a) Time dependence of the first 10 DFT components during an intravital imaging experiment of mouse microglia. This panel shows data for a cell of the "Mobile Cells" type. The x-axis corresponds to time points of the experiment at 60 s time resolution, the y-axis shows the amplitude of the DFT components in arbitrary units (a.u.), whereas the z-axis corresponds to the DFT component from 1 to 10. (b) As in (a) but for a cell of the "Interacting Cells" type. This figure has been modified with permission[8].

Figure 5. (a) The behavior of all 19 DFT components of a cell of the "Mobile Cells" type at the beginning, at the middle and at the end of the experiment. The numbers on the x-axis correspond to the DFT component ID from 1 to 19. The y-axis shows the DFT component amplitude in arbitrary units (a.u.), whilst the z -axis marks the six random rotation angles. (b) Same as in (a) but for a cell of the "Interacting Cells" type. This figure has been modified with permission[8].

DISCUSSION

The identification of potentially pathological conditions using small, intact tissue samples is of high importance. Such techniques will assure a timely response to infectious diseases and aggressive types of cancer. The kinetic and morphological responses of various immune cells, *e.g.,* microglia and macrophages, are characteristic of the immune response of the body. Although in most cases it is not practical or even possible to monitor the kinetic behavior of these cells, it is fairly straightforward to acquire 3-dimensional images to retrieve their shape. Typically, immune cells assume a complex shape in healthy tissue and a much simpler form under inflamed or cancerous conditions[18]. Whilst the time-dependent characteristics of such shape change would add to our understanding of the development of the immune response, using only the 3D shape of a representative group of cells can also be sufficient to determine the healthy or pathological nature of the tissue.

Characterizing the 3-dimensional surface of a cell is not a simple task. The application of spherical harmonics is a way to represent a 3D surface with a relatively large number (50-70) of components[11,12]. In addition, determining the spherical harmonics is computationally expensive; projecting very complex shapes onto the unit sphere is either impossible or very difficult due to the need to apply multiple grids of various fineness on the unit sphere; finally, the meaningful interpretation of the spectra of the spherical harmonics components is far from being trivial.

In our work presented here, we replace the difficult task of direct 3D surface analysis with the much simpler approach of using 2D projections of the original surface to gain sufficient morphological information to identify pathologic conditions. We demonstrated every step of this workflow by using 3D microscopy data from myeloid cells, whilst clearly pointing out that all steps were simple to complete, and the resulting 2-dimensional maps were easy to interpret.

Naturally, a 3D-to-2D projection will lead to information loss about the structure of the surface. In our example dataset of microglia in a mouse cortical tumor model, it was enough to use six angles when creating the 2D projections. However, more complex shapes, or less prominent morphological changes may require that a larger number of projections are created so as to be able to reliably identify cell subgroups with the SOM. For this reason, our approach is designed to be able to generate and analyze any number of projections. Simply by choosing a higher number of projections for more complex shapes, it is possible to scale the information loss to a tolerable minimum. As an example, the interacting cell type in **Figure 4a** and **4b** would require a larger number of projections in order to represent the complex surface properly.

As any approximate method, the hereby proposed workflow had to be tested against the results of a manual classification process of microglia[18]. The results presented earlier confirmed the reliability of the automated workflow. Furthermore, the workflow is more time efficient compared to conventional analysis. The medical expert who classified the microglia cells manually needed approximately 4 weeks for his analysis of the dataset, whereas our workflow needed only about 1 day. The robustness of our approach was also clearly proven by the

reproducibility of the trained SOM to a subset of data that belonged to the same cell type but was not used to train the SOM, as show in **Figure 3c**.

Even though our approach did not consider kinetic information, we examined the effect of timing on the DFT-based shape analysis. The most typical example for time-dependent behavior was found amongst the mobile cell population, where the contribution from the higher indexed DFT components was clearly observable, as in **Figure 4a**. This calls attention to the importance of utilizing a high enough number of DFT components when dealing with cell types that are likely to behave in a very time-dependent manner. Due to the automated nature and high execution speed of our software tools, the increased number of DFT components and projections will increase the precision and reliability of the results, whilst they will not appreciably hinder the computational performance.

DISCLOSURES

The authors declare that they have no competing financial interests.

ACKNOWLEDGMENTS

The authors thank Benjamin Krause for the fruitful discussion and his support. The authors further thank Robert Günther for his assistance with the live cell microscopy.
The work was supported by the DFG financial support NI1167/3–1 (JIMI) to R.N. and Z.C., C01 in TRR130 to R.N. and SFB633, TRR130, Exc257 to A.E.H. and J.B.S. The BfR provided intramural support SFP1322-642 for F.L.K and A.L.

REFERENCES:

1 Masedunskas, A. *et al.* Intravital microscopy: a practical guide on imaging intracellular structures in live animals. *Bioarchitecture.* **2** (5), 143-157 (2012).

2 Niesner, R. A. & Hauser, A. E. Recent advances in dynamic intravital multi-photon microscopy. *Cytometry A.* **79** (10), 789-798 (2011).

3 Ho, S. Y. *et al.* NeurphologyJ: an automatic neuronal morphology quantification method and its application in pharmacological discovery. *BMC Bioinformatics.* **12,** 230 (2011).

4 Yin, Z. *et al.* A screen for morphological complexity identifies regulators of switch-like transitions between discrete cell shapes. *Nature Cell Biology.* **15** (7), 860 (2013).

5 Yu, H. Y., Lim, K. P., Xiong, S. J., Tan, L. P. & Shim, W. Functional Morphometric Analysis in Cellular Behaviors: Shape and Size Matter. *Advanced Healthcare Materials.* **2** (9) (2013).

6 Johnson, G. R., Buck, T. E., Sullivan, D. P., Rohde, G. K. & Murphy, R. F. Joint modeling of cell and nuclear shape variation. *Molecular Biology of the Cell.* **26** (22), 4046-4056 (2015).

7 Wang, S.-H., Cheng, H., Phillips, P. & Zhang, Y.-D. Multiple Sclerosis Identification Based on Fractional Fourier Entropy and a Modified Jaya Algorithm. *Entropy.* **20** (4), 254 (2018).

8 Kriegel, F. L. *et al.* Cell shape characterization and classification with discrete Fourier transforms and self-organizing maps. *Cytometry Part A.* **93** (3), 323-333 (2017).

9 Styner, M. *et al.* Framework for the Statistical Shape Analysis of Brain Structures using SPHARM-PDM. *Insight Journal.* (1071), 242-250 (2006).

10 El-Baz, A. *et al.* 3D shape analysis for early diagnosis of malignant lung nodules. *Medical Image Computing and Computer Assisted Intervention.* **14** (Pt 3), 175-182 (2011).

11 Williams, E. L., El-Baz, A., Nitzken, M., Switala, A. E. & Casanova, M. F. Spherical harmonic analysis of cortical complexity in autism and dyslexia. *Translational Neuroscience.* **3** (1), 36-40 (2012).
12 Kruggel, F. Robust parametrization of brain surface meshes. *Medical Image Analysis.* **12** (3), 291-299 (2008).
13 Schindelin, J. *et al.* Fiji: an open-source platform for biological-image analysis. *Nature Methods.* **9** (7), 676-682 (2012).
14 Kohonen, T. Essentials of the self-organizing map. *Neural Networks.* **37,** 52-65 (2013).
15 Andrey P, B. T. Adaptive Active Contours in *ImageJ user and developer conference* (Luxembourg, 2006).
16 Burger, W. & Burge, M. J. *Principles of Digital Image Processing*. (Springer-Verlag, 2013).
17 Lestrel, P. E. *Fourier Descriptors and their Applications in Biology*. (Cambridge University Press, 2008).
18 Bayerl, S. H. *et al.* Time lapse *in vivo* microscopy reveals distinct dynamics of microglia-tumor environment interactions-a new role for the tumor perivascular space as highway for trafficking microglia. *Glia.* **64** (7), 1210-1226 (2016).

Figure 1

Click here to download Figure Figure1_Kriegel_etal_2018.eps

Microscopy data

Step 1: 3D surface reconstruction with Imaris

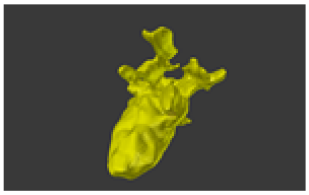

3D surface as vrml file

Step 2: Automated rotations to generate 2D projections in Blender

tiff images

Step 3: DFT calculations utilizing Fiji and SHADE Plugin

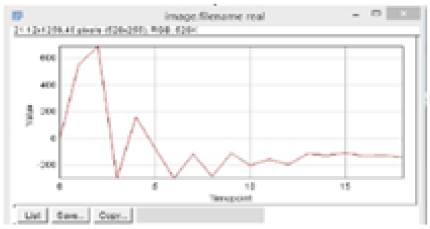

csv files

Step 4: SOM analysis with Matlab

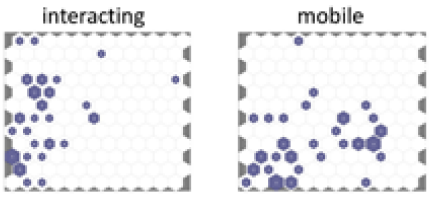

Data clustering based on the shape

Figure 2

Click here to download Figure Figure_2_Kriegel_etal_2018.eps

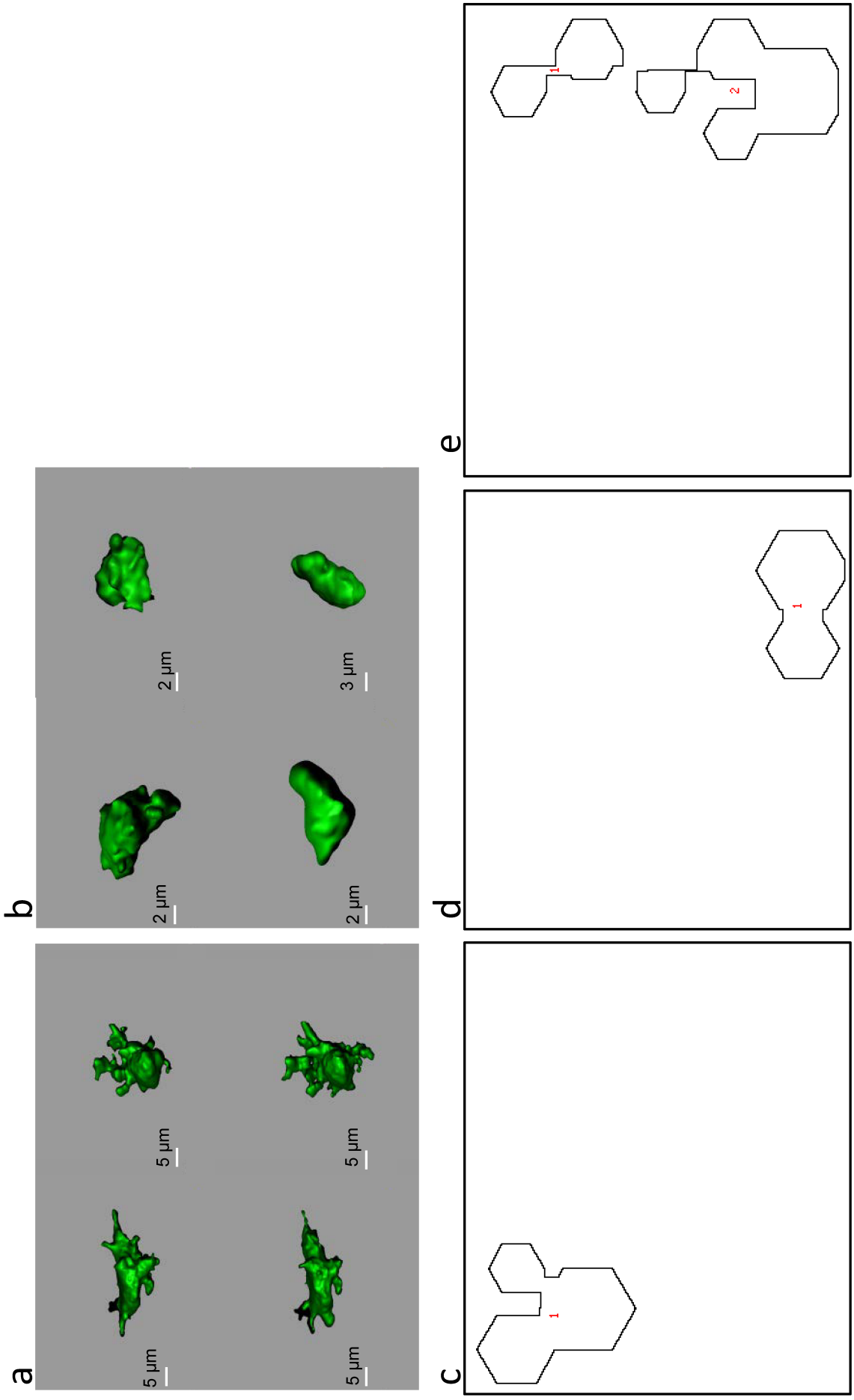

Figure 3

a

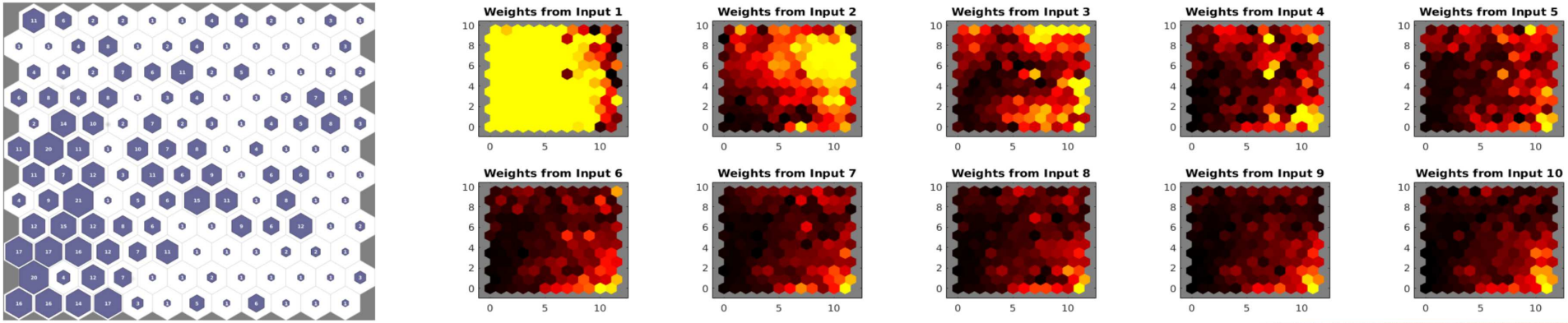

b

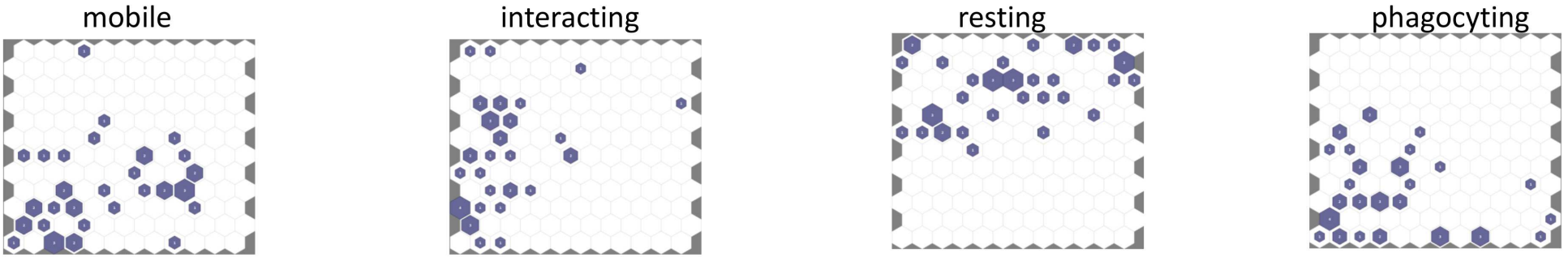

c

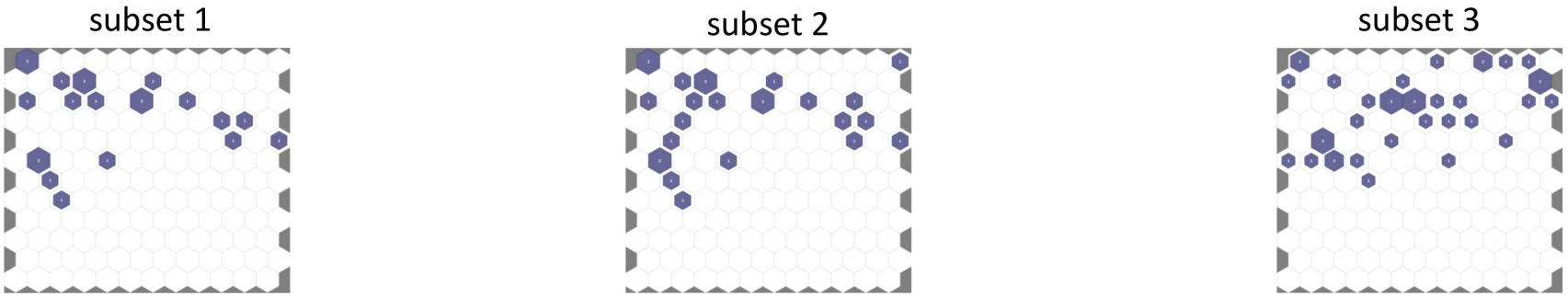

Click here to download Figure Figure_3_Kriegel_etal_2018.eps

Figure 4

Click here to download Figure Figure_4_Kriegel_etal_2018.eps

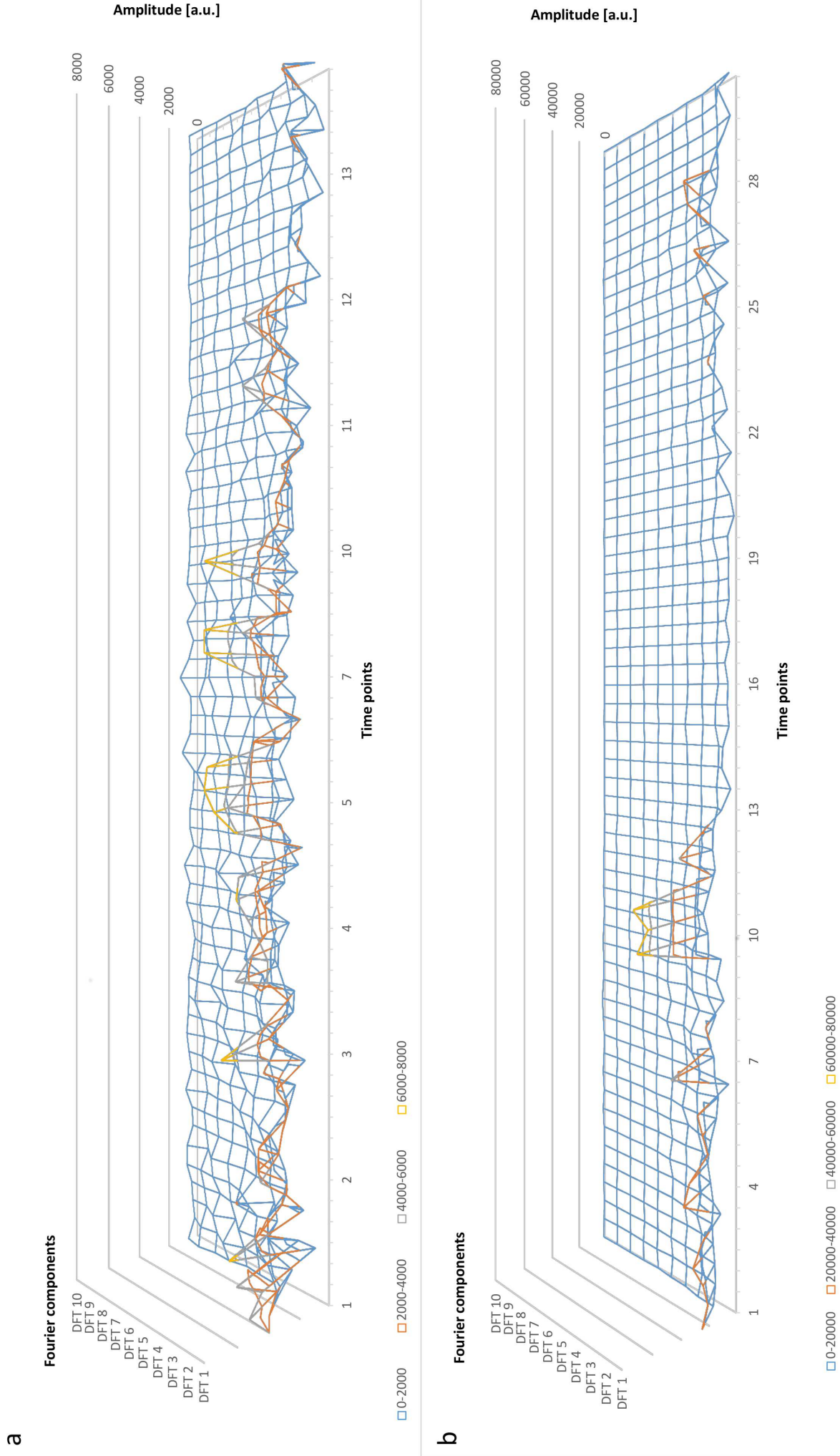

Figure 5

Click here to download Figure Figure_5_Kriegel_etal_2018.eps

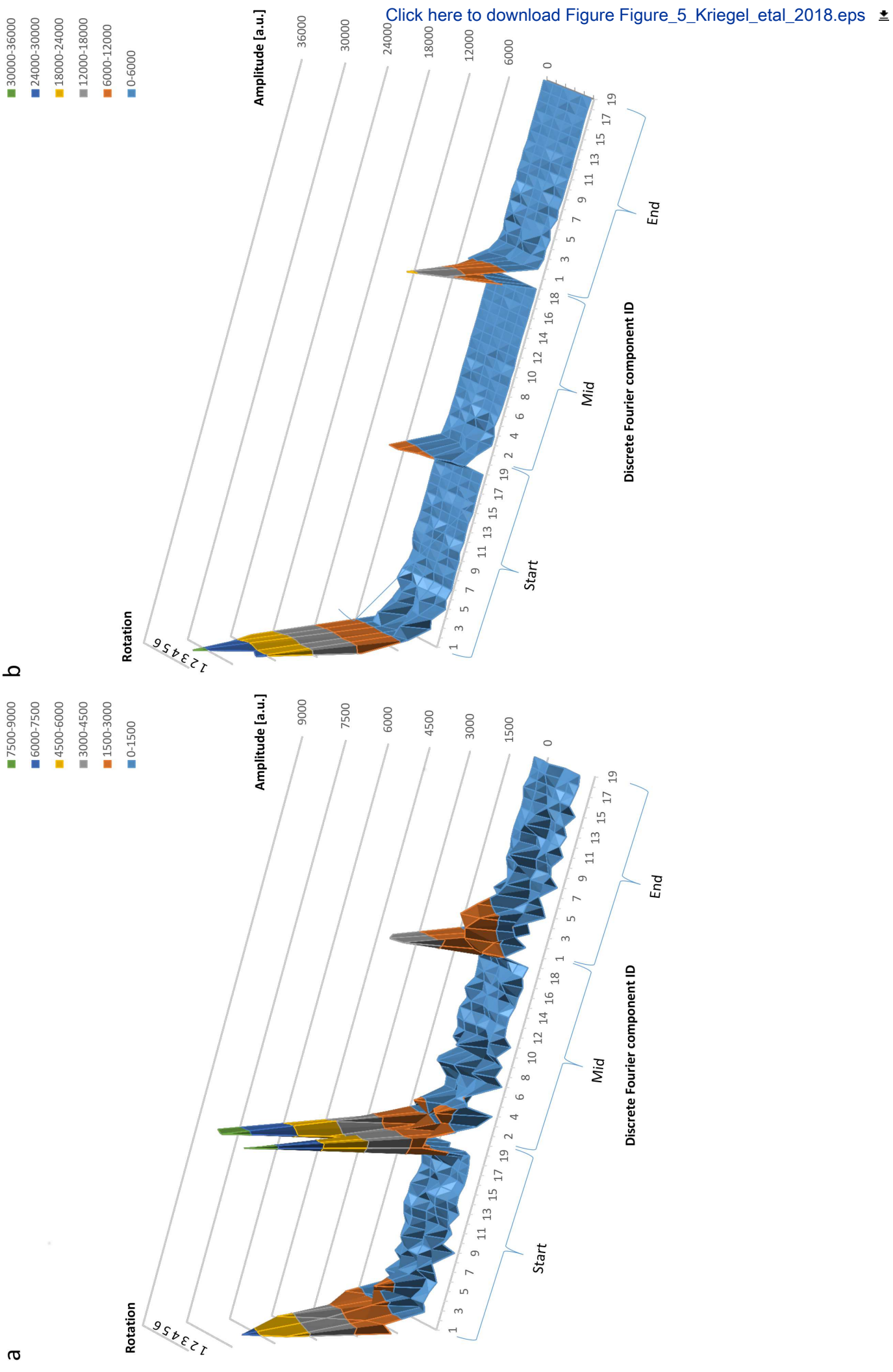

Video_Imaris_Workflow

Click here to access/download

Video or Animated Figure

Video_Imaris_Workflow_new.flv

Video_SHADE_Workflow

Click here to access/download

Video or Animated Figure

Video_SHADE_Workflow.flv

Video_SOM_train_Workflow

Click here to access/download

Video or Animated Figure

Video_SOM_train_Workflow.flv

Video_SOM_apply_Workflow

Click here to access/download

Video or Animated Figure

Video_SOM_apply_Workflow.flv

Video_Blender_fromBlender_Workflow

Click here to access/download

Video or Animated Figure

Video_Blender_fromBlender_Workflow.flv

Video_Blender_fromPython_Workflow

Click here to access/download

Video or Animated Figure

Video_Blender_fromPython_Workflow.flv

Click here to download Table of Materials
JoVE_Materials_Kriegel_etal_2018_revised.xls

Name of Material/ Equipment

Imaris 9.1.2, software
Blender 2.75a, software
Fiji /ImageJ, software
MATLAB
MATLAB Machine Learning kit
Fiji plugins: SHADE
Fiji plugins: ActiveContour
Computer

Company	Catalog Number
Bitplane, Zürich, Switzerland	v.9.1.2
https://www.blender.org/	v.2.75a
https://fiji.sc/	ImageJ v.1.52b
MathWorks, www. mathworks.com	R2017b
MathWorks, www. mathworks.com	R2017b
https://github.com/zcseresn/ShapeAnalysis	v.1.0
http://imagejdocu.tudor.lu/doku.php?id=plugin:segmentation:active_contour:start	absnake2
Any	NA

Comments/Description

3D image reconstruction and surface generation; this was used by us!
3D and 4D open source animation software; 2.75a is the required version for this Python
Open source multi-D image analysis toolkit
General computational mathematical software
Can only be used together with MATLAB

See Imaris instructions for minimum computer requirements

Author License Agreement (ALA)
Click here to download Author License Agreement (ALA)
Author_License_Agreement_Kriegel_etal_2018.pdf

jove JOURNAL OF VISUALIZED EXPERIMENTS
1 Alewife Center #200
Cambridge, MA 02140
tel. 617.945.9051
www.jove.com

ARTICLE AND VIDEO LICENSE AGREEMENT

Title of Article: Morphology-based distinction between healthy and pathological cells utilizing Fourier transforms and Self-Organizing Maps

Author(s): Kriegel FL, Köhler R, Bayat-Sarmadi J, Bayerl S, Hauser AE, Niesner R, Luch A, Cseresnyes Z.

Item 1 (check one box): The Author elects to have the Materials be made available (as described at http://www.jove.com/author) via: [ ] Standard Access [X] Open Access

Item 2 (check one box):

[X] The Author is NOT a United States government employee.

[ ] The Author is a United States government employee and the Materials were prepared in the course of his or her duties as a United States government employee.

[ ] The Author is a United States government employee but the Materials were NOT prepared in the course of his or her duties as a United States government employee.

ARTICLE AND VIDEO LICENSE AGREEMENT

1. Defined Terms. As used in this Article and Video License Agreement, the following terms shall have the following meanings: "**Agreement**" means this Article and Video License Agreement; "**Article**" means the article specified on the last page of this Agreement, including any associated materials such as texts, figures, tables, artwork, abstracts, or summaries contained therein; "**Author**" means the author who is a signatory to this Agreement; "**Collective Work**" means a work, such as a periodical issue, anthology or encyclopedia, in which the Materials in their entirety in unmodified form, along with a number of other contributions, constituting separate and independent works in themselves, are assembled into a collective whole; "**CRC License**" means the Creative Commons Attribution-Non Commercial-No Derivs 3.0 Unported Agreement, the terms and conditions of which can be found at: http://creativecommons.org/licenses/by-nc-nd/3.0/legalcode; "**Derivative Work**" means a work based upon the Materials or upon the Materials and other pre-existing works, such as a translation, musical arrangement, dramatization, fictionalization, motion picture version, sound recording, art reproduction, abridgment, condensation, or any other form in which the Materials may be recast, transformed, or adapted; "**Institution**" means the institution, listed on the last page of this Agreement, by which the Author was employed at the time of the creation of the Materials; "**JoVE**" means MyJove Corporation, a Massachusetts corporation and the publisher of *The Journal of Visualized Experiments;* "**Materials**" means the Article and / or the Video; "**Parties**" means the Author and JoVE; "**Video**" means any video(s) made by the Author, alone or in conjunction with any other parties, or by JoVE or its affiliates or agents, individually or in collaboration with the Author or any other parties, incorporating all or any portion of the Article, and in which the Author may or may not appear.

2. Background. The Author, who is the author of the Article, in order to ensure the dissemination and protection of the Article, desires to have the JoVE publish the Article and create and transmit videos based on the Article. In furtherance of such goals, the Parties desire to memorialize in this Agreement the respective rights of each Party in and to the Article and the Video.

3. Grant of Rights in Article. In consideration of JoVE agreeing to publish the Article, the Author hereby grants to JoVE, subject to **Sections 4** and **7** below, the exclusive, royalty-free, perpetual (for the full term of copyright in the Article, including any extensions thereto) license (a) to publish, reproduce, distribute, display and store the Article in all forms, formats and media whether now known or hereafter developed (including without limitation in print, digital and electronic form) throughout the world, (b) to translate the Article into other languages, create adaptations, summaries or extracts of the Article or other Derivative Works (including, without limitation, the Video) or Collective Works based on all or any portion of the Article and exercise all of the rights set forth in (a) above in such translations, adaptations, summaries, extracts, Derivative Works or Collective Works and (c) to license others to do any or all of the above. The foregoing rights may be exercised in all media and formats, whether now known or hereafter devised, and include the right to make such modifications as are technically necessary to exercise the rights in other media and formats. If the "Open Access" box has been checked in **Item 1** above, JoVE and the Author hereby grant to the public all such rights in the Article as provided in, but subject to all limitations and requirements set forth in, the CRC License.

4. Retention of Rights in Article. Notwithstanding the exclusive license granted to JoVE in **Section 3** above, the Author shall, with respect to the Article, retain the non-exclusive right to use all or part of the Article for the non-commercial purpose of giving lectures, presentations or teaching classes, and to post a copy of the Article on the Institution's website or the Author's personal website, in each case provided that a link to the Article on the JoVE website is provided and notice of JoVE's copyright in the Article is included. All non-copyright intellectual property rights in and to the Article, such as patent rights, shall remain with the Author.

5. Grant of Rights in Video – Standard Access. This **Section 5** applies if the "Standard Access" box has been checked in **Item 1** above or if no box has been checked in **Item 1** above. In consideration of JoVE agreeing to produce, display or otherwise assist with the Video, the Author hereby acknowledges and agrees that, Subject to **Section 7** below, JoVE is and shall be the sole and exclusive owner of all rights of any nature, including, without limitation, all copyrights, in and to the Video. To the extent that, by law, the Author is deemed, now or at any time in the future, to have any rights of any nature in or to the Video, the Author hereby disclaims all such rights and transfers all such rights to JoVE.

6. Grant of Rights in Video – Open Access. This **Section 6** applies only if the "Open Access" box has been checked in **Item 1** above. In consideration of JoVE agreeing to produce, display or otherwise assist with the Video, the Author hereby grants to JoVE, subject to **Section 7** below, the exclusive, royalty-free, perpetual (for the full term of copyright in the Article, including any extensions thereto) license (a) to publish, reproduce, distribute, display and store the Video in all forms, formats and media whether now known or hereafter developed (including without limitation in print, digital and electronic form) throughout the world, (b) to translate the Video into other languages, create adaptations, summaries or extracts of the Video or other Derivative Works or Collective Works based on all or any portion of the Video and exercise all of the rights set forth in (a) above in such translations, adaptations, summaries, extracts, Derivative Works or Collective Works and (c) to license others to do any or all of the above. The foregoing rights may be exercised in all media and formats, whether now known or hereafter devised, and include the right to make such modifications as are technically necessary to exercise the rights in other media and formats. For any Video to which this Section 6 is applicable, JoVE and the Author hereby grant to the public all such rights in the Video as provided in, but subject to all limitations and requirements set forth in, the CRC License.

7. Government Employees. If the Author is a United States government employee and the Article was prepared in the course of his or her duties as a United States government employee, as indicated in **Item 2** above, and any of the licenses or grants granted by the Author hereunder exceed the scope of the 17 U.S.C. 403, then the rights granted hereunder shall be limited to the maximum rights permitted under such statute. In such case, all provisions contained herein that are not in conflict with such statute shall remain in full force and effect, and all provisions contained herein that do so conflict shall be deemed to be amended so as to provide to JoVE the maximum rights permissible within such statute.

8. Likeness, Privacy, Personality. The Author hereby grants JoVE the right to use the Author's name, voice, likeness, picture, photograph, image, biography and performance in any way, commercial or otherwise, in connection with the Materials and the sale, promotion and distribution thereof. The Author hereby waives any and all rights he or she may have, relating to his or her appearance in the Video or otherwise relating to the Materials, under all applicable privacy, likeness, personality or similar laws.

9. Author Warranties. The Author represents and warrants that the Article is original, that it has not been published, that the copyright interest is owned by the Author (or, if more than one author is listed at the beginning of this Agreement, by such authors collectively) and has not been assigned, licensed, or otherwise transferred to any other party. The Author represents and warrants that the author(s) listed at the top of this Agreement are the only authors of the Materials. If more than one author is listed at the top of this Agreement and if any such author has not entered into a separate Article and Video License Agreement with JoVE relating to the Materials, the Author represents and warrants that the Author has been authorized by each of the other such authors to execute this Agreement on his or her behalf and to bind him or her with respect to the terms of this Agreement as if each of them had been a party hereto as an Author. The Author warrants that the use, reproduction, distribution, public or private performance or display, and/or modification of all or any portion of the Materials does not and will not violate, infringe and/or misappropriate the patent, trademark, intellectual property or other rights of any third party. The Author represents and warrants that it has and will continue to comply with all government, institutional and other regulations, including, without limitation all institutional, laboratory, hospital, ethical, human and animal treatment, privacy, and all other rules, regulations, laws, procedures or guidelines, applicable to the Materials, and that all research involving human and animal subjects has been approved by the Author's relevant institutional review board.

10. JoVE Discretion. If the Author requests the assistance of JoVE in producing the Video in the Author's facility, the Author shall ensure that the presence of JoVE employees, agents or independent contractors is in accordance with the relevant regulations of the Author's institution. If more than one author is listed at the beginning of this Agreement, JoVE may, in its sole discretion, elect not take any action with respect to the Article until such time as it has received complete, executed Article and Video License Agreements from each such author. JoVE reserves the right, in its absolute and sole discretion and without giving any reason therefore, to accept or decline any work submitted to JoVE. JoVE and its employees, agents and independent contractors shall have

jove JOURNAL OF VISUALIZED EXPERIMENTS
1 Alewife Center #200
Cambridge, MA 02140
tel. 617.945.9051
www.jove.com

ARTICLE AND VIDEO LICENSE AGREEMENT

full, unfettered access to the facilities of the Author or of the Author's institution as necessary to make the Video, whether actually published or not. JoVE has sole discretion as to the method of making and publishing the Materials, including, without limitation, to all decisions regarding editing, lighting, filming, timing of publication, if any, length, quality, content and the like.

11. Indemnification. The Author agrees to indemnify JoVE and/or its successors and assigns from and against any and all claims, costs, and expenses, including attorney's fees, arising out of any breach of any warranty or other representations contained herein. The Author further agrees to indemnify and hold harmless JoVE from and against any and all claims, costs, and expenses, including attorney's fees, resulting from the breach by the Author of any representation or warranty contained herein or from allegations or instances of violation of intellectual property rights, damage to the Author's or the Author's institution's facilities, fraud, libel, defamation, research, equipment, experiments, property damage, personal injury, violations of institutional, laboratory, hospital, ethical, human and animal treatment, privacy or other rules, regulations, laws, procedures or guidelines, liabilities and other losses or damages related in any way to the submission of work to JoVE, making of videos by JoVE, or publication in *JoVE* or elsewhere by JoVE. The Author shall be responsible for, and shall hold JoVE harmless from, damages caused by lack of sterilization, lack of cleanliness or by contamination due to the making of a video by JoVE its employees, agents or independent contractors. All sterilization, cleanliness or decontamination procedures shall be solely the responsibility of the Author and shall be undertaken at the Author's expense. All indemnifications provided herein shall include JoVE's attorney's fees and costs related to said losses or damages. Such indemnification and holding harmless shall include such losses or damages incurred by, or in connection with, acts or omissions of JoVE, its employees, agents or independent contractors.

12. Fees. To cover the cost incurred for publication, JoVE must receive payment before production and publication the Materials. Payment is due in 21 days of invoice. Should the Materials not be published due to an editorial or production decision, these funds will be returned to the Author. Withdrawal by the Author of any submitted Materials after final peer review approval will result in a US$1,200 fee to cover pre-production expenses incurred by JoVE. If payment is not received by the completion of filming, production and publication of the Materials will be suspended until payment is received.

13. Transfer, Governing Law. This Agreement may be assigned by JoVE and shall inure to the benefits of any of JoVE's successors and assignees. This Agreement shall be governed and construed by the internal laws of the Commonwealth of Massachusetts without giving effect to any conflict of law provision thereunder. This Agreement may be executed in counterparts, each of which shall be deemed an original, but all of which together shall be deemed to me one and the same agreement. A signed copy of this Agreement delivered by facsimile, e-mail or other means of electronic transmission shall be deemed to have the same legal effect as delivery of an original signed copy of this Agreement.

A signed copy of this document must be sent with all new submissions. Only one Agreement required per submission.

CORRESPONDING AUTHOR:

Name:	Zoltan Cseresnyes
Department:	Applied Systems Biology
Institution:	Hans-Knöll Institute, Jena, Germany
Article Title:	Morphology-based distinction between healthy and pathological cells utilizing Fourier transforms and Self-Organizing Maps
Signature:	Date: 31 May, 2018

Please submit a signed and dated copy of this license by one of the following three methods:

1) Upload a scanned copy of the document as a pfd on the JoVE submission site;
2) Fax the document to +1.866.381.2236;
3) Mail the document to JoVE / Attn: JoVE Editorial / 1 Alewife Center #200 / Cambridge, MA 02139

For questions, please email submissions@jove.com or call +1.617.945.9051

Rebuttal Letter
Click here to download Rebuttal Letter
Response_to_Editor_and_Reviewers_Kreiegel_etal_JoVE2018.d

All changes made by the authors to the main text of the manuscript are highlighted in purple!

Editorial Comments:

1. Please take this opportunity to thoroughly proofread the manuscript to ensure that there are no spelling or grammar issues. The JoVE editor will not copy-edit your manuscript and any errors in the submitted revision may be present in the published version.

We thank the editor for this important note. We would also like to mention that we were surprised to learn that proofreading is not included in the rather high publication cost. At the same time, we have taken the opportunity to carefully check the text for spelling and grammar. We hope that we didn't miss any error.

2. JoVE cannot publish manuscripts containing commercial language. This includes trademark symbols (™), registered symbols (®), and company names before an instrument or reagent. Please remove all commercial language from your manuscript and use generic terms instead. All commercial products should be sufficiently referenced in the Table of Materials and Reagents. For example: Imaris, Blender, etc.

We have taken this important note from the editor into account and incorporated all commercially used programs into the material and methods part. Furthermore, we have removed all commercial language from the text and inserted general descriptions of the required functions instead (see also marked passages in the manuscript). At the same time, the Blender framework should probably be not considered a commercial product (it is a free access, open source framework), thus we left the Blender name in the text. Moreover, our Python script is very specific to the Blender environment, thus the 3D-to-2D projection process can't be described in general terms.

3. Please ensure that all text in the protocol section is written in the imperative tense as if telling someone how to do the technique (e.g., "Do this," "Ensure that," etc.). The actions should be described in the imperative tense in complete sentences wherever possible. Avoid usage of phrases such as "could be," "should be," and "would be" throughout the Protocol. Any text that cannot be written in the imperative tense may be added as a "Note." However, notes should be concise and used sparingly. Please include all safety procedures and use of hoods, etc.

We thank the editor for this helpful hint. We have now reworked the Protocol part into the requested format and we hope that it meets the requirements of the journal. In addition, we have worked on the text in order to depict the individual steps of the protocol more precisely and comprehensibly.

4. The Protocol should contain only action items that direct the reader to do something. Please move the discussion about the protocol to the Discussion.

We have decided to completely remove most of the non-directional parts of the protocol from the text in order to guarantee an easier reproducibility of the protocol. We thank the editor for this advice.

5. The Protocol should be made up almost entirely of discrete steps without large paragraphs of text between sections. Please simplify the Protocol so that individual steps contain only 2-3 actions per step and a maximum of 4 sentences per step.

The Protocol part has been revised according to the notes of the editor. We have replaced the long text passages with shorter and more concise formulations. Additionally, we now use the NOTE function of the journal to give important hints without affecting the clarity of the protocol.

6. It would help to have example data that can be provided with the article. We cannot film a general protocol so a specific example will allow us to have specific values and parameters to use in the video.

We thank the editor for this important note. For the demonstration of the training process and the classification of the shape data using SOM, we have already uploaded a corresponding example data set to github and referenced it in the text. For the 3D reconstruction of the microscopy data and the calculation of the DFT components, we now also provide sample data sets. The download instructions have been provided at the appropriate sections of the protocol part.

7. Please highlight 2.75 pages or less of the Protocol (including headings and spacing) that identifies the essential steps of the protocol for the video, i.e., the steps that should be visualized to tell the most cohesive story of the Protocol. Remember that non-highlighted Protocol steps will remain in the manuscript, and therefore will still be available to the reader.

Due to the revision of the protocol part we took the editor's critics to heart and now only marked the most important steps. We hope that this will make the workflow easy to understand and follow. Our current marked protocol length is under 2 pages.

8. Please ensure that the highlighted steps form a cohesive narrative with a logical flow from one highlighted step to the next. Please highlight complete sentences (not parts of sentences). Please ensure that the highlighted part of the step includes at least one action that is written in imperative tense.

We have checked and revised our protocol with regard to the comprehensibility of the individual steps and the reproducibility of the overall context and hope that we have successfully implemented the editor's suggestions.

9. Please do not highlight the python script steps (4.2, etc.).

During the protocol review process, we realized that the points marked under 4.2., describing Matlab functions to examine the neural network’s topology, would only confuse the reader. We have therefore removed the markings in the corresponding places and converted most of the passages into NOTES.

10. Please obtain explicit copyright permission to reuse any figures from a previous publication. Explicit permission can be expressed in the form of a letter from the editor or a link to the editorial policy that allows re-prints. Please upload this information as a .doc or .docx file to your Editorial Manager

account. The Figure must be cited appropriately in the Figure Legend, i.e. “This figure has been modified from [citation].”

We obtained a letter from the copyright handler of Cytometry A by following our Cytometry A editor’s instructions, and we uploaded the approval note as a PDF file to our editorial manager account during the original submission process. The citation of the figures was changed according to the editor’s suggestions.

11. Please include an Acknowledgements section, containing any acknowledgments and all funding sources for this work.

We thank the editor for spotting our mistake. We added an Acknowledgements sections to our manuscript and acknowledged colleagues and stated all funding sources for the presented work.

12. Please do not abbreviate journal titles.

We reworked the reference list of the manuscript according to the editor’s suggestion.

Reviewer 1:

1. The shape analysis is very effective. Why use SOM? Do you consider to use deep learning method?

We appreciate the reviewer’s feedback about the effectiveness of our shape analysis. During the implementation of our research project we had some discussions about the classification algorithm to be used. We chose SOM because it had distinct advantages for our data set. Due to the 2D overview of clustering, SOM results are very easy to interpret and changes in the hit- and distance-map patterns can be quickly identified by the user. A preliminary tagging of the data by the user to train the algorithm is not necessary for SOM, since SOM belongs to the group of unsupervised learning methods. In addition, such tagging of the dataset by the user may not always be objectively feasible. SOMs have the advantage over other systems that connections that remain hidden to the human observer can be identified by the algorithm. A very good alternative to SOMs are deep learning algorithms, as pointed out by the reviewer. However, deep learning algorithms need a large training dataset in order to function properly. Such large and tagged dataset was not available to us, thus we chose SOM as a valid alternative for our specific problem. Nevertheless, with a larger tagged training dataset, deep learning algorithms can be more efficient and successful than SOM. With the advent of large voluntary image datasets, this goal should be achievable in the not too distant future.

2. Line 242, why not use the inline function "selforgmap" provided by Matlab?

We appreciate the reviewers suggestion about the Matlab inline function. We actually already use this function in the provided Matlab script (line 72) to initiate the SOM. We provided this Matlab script for inexperienced users to simplify the task of training an SOM. However, the utilization of the above-mentioned inline command is indeed sufficient for more experienced users.

3. Line 253, why 2,000 iterations? What is the effect of setting other values of maximum iteration number?

The SOM starts to learn to distinguish between the various feature vector spaces only after the proper number of iterations. At the same time, too many iterations will result in “over-learning”, i.e., where the number of highly responsive artificial neurons will drop, thus the SOM would lose its functionality. We tested various numbers of iterations and found that after 2000 iterations the shape-based SOM learning pattern has stabilized. We recommend using 2000 iterations for systems similar to ours.

4. From 303, there are too many question marks in the equation. Can you check them?

In the final pdf version generated by JoVE at the end of the original submission process we cannot see any question marks in the Equation section and everything looks fine. However, we reassessed this part to make sure not to overlook any mistakes.

5. The results are quite good. One paper may help the readers understand your paper, and may be mentioned, see "Multiple sclerosis identification based on fractional Fourier entropy and a modified Jaya algorithm"

We appreciate the reviewer’s feedback about our proposed methodology and we now include a reference to the paper that the reviewer mentioned.

Reviewer 2:

Major Concerns:

1. In its current version the protocol appears not to be very user friendly. Firstly it requires 4 different softwares, 2 of which are commercial. Secondly, the delivered scripts should still be edited by the user if required (step 2.3 and 4.1.5 of the protocol). The protocol would be easier to use if the scripts are integrated together. Ideally the user would run Imaris for the surfaces and then run a custom Matlab GUI that invisibly calls the python and fiji scripts before running the SOM (with options for train and test). This may not be feasible, but at least the Blender and Fiji scripts should be integrated together. Also any of the user-defined parameters should be changeable in the GUI instead of within the scripts. In this way the users of the protocol do not need to know how to use 4 different programs and get used to reading scripts.

We thank the reviewer for the suggestion of integrating the script together and adding a GUI to customize the parameters for the software. We plan to work on the integration of Imaris and Matlab together with the Python script and the Fiji code and hope to make this available at a not too distant future time point. We already implemented a GUI for the Blender part to allow the user to change parameters without having to edit the script. We adjusted the Protocol accordingly.

2. The introduction to the protocol as well as the steps from 1 - 4.2.2.3 are not easy to follow. It could be written more to the point. The introductory text can be integrated in the bullet points and the different steps need to have conclusive titles. Thus the protocol could be followed step by step.

We followed the reviewer's suggestion and transformed the introduction part of the protocol into bullet points. We also reworked the protocol and used a more concise language. Moreover, we transformed several steps into Notes and we hope that the protocol can be now be followed more easily.

3. The projections of the cells are obtained in Blender (Step 2). The authors advice to use at least 6 different looking angles for the projections and more if the shape is complex. How can the user know how many projections should be made? Is there a way to check that there is no under-sampling of the shape?

We tested various numbers of rotation and found that for the precise description of microglia six rotation were satisfactory. We would not recommend using a lower value for microglia (or other, similarly complex shapes), in order to avoid loss of information. The number of rotations needed may vary for each cell type depending on the size and complexity of the shape of the cell. A higher number of rotations will lead to a more precise transformation of the 3D shape into 2D. A simple way to check the necessary amount of rotations is depicted in Figure 5. If the DFT components' amplitude does not change with an increased number of rotations, we assume that we don't gain any further information about the shape by having more rotations.

4. To obtain the perimeter of the projections of the cells, the authors use the active contour algorithm in Fiji (step 3). Since the data is already segmented and appears to be a binary (only zeros and ones) 8-bit image, couldn't the authors make use of an easier and less computationally expensive method, like an edge-detector (Sobel filter)?

The reviewer correctly states that an edge detecting algorithm such as the Sobel filter can be successfully applied on binarized datasets. However, most of the edge-finder algorithms have difficulties if the shape of the object has holes in it. This can be sorted out if a filter is applied before or after the Sobel filter, in order to get rid of the "false" edges (holes in the shape) that were found. We found the Snake algorithm simpler in this regard, because it starts from the outside of the cell and is able to detect the outline and invaginations of the cell membrane in a reliable manner even if the shape has hole(s) in it, without the need for an additional filter.

5. In the 'representative results' section (Fig. 3b and c) it is unclear whether testing the trained-SOM was done on cells that were included in the training dataset. If so, no real conclusions can be made on the performance of the SOM from the results on test-data. The use of the word 'subset' (l. 355, 356, 363 and 462) implies that the test-set are part of the training dataset although it could also mean that they are another part of the entire dataset. It needs to be clearly stated in the text on which data the SOM is trained and tested and what is shown in the figures.

We thank the reviewer for spotting this imprecise wording on our behalf. Different datasets were used for the training and for the later classification with the trained SOM. We changed the text accordingly to clarify that the cells which were tested on the SOM were not included in the initial training dataset of the SOM.

6. The results of the time-dependent cell shape analysis show the changes over time of the DFT of the cell shapes of 2 types of cells (Fig.4). Since the protocol is explicitly useful for data without time

component, does a trained SOM classify these cells at single time-points to the groups they belong to (resp. 'Mobile' and 'Interacting')? That would confirm that the proposed method is able to distinguish between cell types in single time points.

Indeed the trained SOM was in our case capable of classifying the cells from single time points into the group that the medical expert appointed. We agree with the reviewer that our method is able to distinguish cells in single time points.

7. In the discussion (l. 459-461) the authors mention that the method is very fast which argues for 'superiority', but no timing nor any comparison to other methods is given.

We appreciate the reviewer comment about the missing performance characterization. Regarding the timing aspect, we can provide an example: the medical expert who classified the cells manually needed approximately 4 weeks for his analysis of the dataset, whereas our workflow needed only about 1 day, including all steps. We added a corresponding section to the discussion.

8. The videos have no voice-over that explains what is being done. Addition of an explanatory voice could be useful to follow better what is being done.

The videos were only provided by us to clarify our approach to the reviewers, as suggested by the editor. These videos will be re-shot professionally, using the voice-over of an actor provided by JoVE.

Minor Concerns:

1. The introduction could be more explanatory, for example an explanation of SOM could be added as well as an explanation of the 20 DFT components that are talked of later on.

Following the reviewers suggestion we added explanatory parts in the introduction for DFT and SOM.

2. In the list of equipment Matlab & Machine Learning Toolbox are missing

We thank the reviewer for spotting our mistake. We added the entries accordingly in the Materials and Methods section.

3. In l.351/352 the reference to Figure 2a-d appears incorrect: a-b are examples of cell forms (as observed by expert) but c-e are results of SOM

We thank the reviewer for spotting our mistake. We corrected the figure legend according to the reviewer's suggestion.

4. In l.259, protocol part 2.1.5, the authors speak of a Python script where the paragraph describes the Matlab part of the protocol.

We once again thank the reviewer for spotting our error. We fixed this issue in the text.

5. -7.

We are sorry about the inconvenience caused by the faulty video “Video_Blender_fromBlender_Workflow.flv”, it has now been replaced with an updated video using the GUI-based Python script built into Blender “AutoRotate_v2.0.blend”. We also recreated the video corresponding to the GUI-based Python script that we newly added to this work (“Video_Blender_fromPython_Workflow.flv” The rest of the videos seem to play flawlessly in VLC. Please also note that these videos were only provided to clarify our approach to the reviewers (as suggested by the editor). We do not plan to publish these videos, rather they will be shot professionally including proper voice-over by the JoVE staff. At this stage of the revision we are not referring to the videos anymore in the manuscript. Nevertheless we also uploaded the updated versions of the videos for the Reviewers’ and Editor’s convenience.

JOHN WILEY AND SONS LICENSE TERMS AND CONDITIONS

May 22, 2018

This Agreement between Dr. Zoltan Cseresnyes ("You") and John Wiley and Sons ("John Wiley and Sons") consists of your license details and the terms and conditions provided by John Wiley and Sons and Copyright Clearance Center.

License Number	4354140023072
License date	May 22, 2018
Licensed Content Publisher	John Wiley and Sons
Licensed Content Publication	Cytometry Part A
Licensed Content Title	Cell shape characterization and classification with discrete Fourier transforms and self-organizing maps
Licensed Content Date	Oct 27, 2017
Licensed Content Pages	11
Type of use	Journal/Magazine
Requestor type	Author of this Wiley article
Is the reuse sponsored by or associated with a pharmaceutical or medical products company?	no
Format	Electronic
Portion	Figure/table
Number of figures/tables	5
Original Wiley figure/table number(s)	Figure 3 Figure 5 Figure 6 Figure 7 Figure 8
Will you be translating?	No
Circulation	10000
Title of new article	Morphology-based distinction between healthy and pathological cells utilizing Fourier transforms and Self-Organizing Maps
Publication the new article is in	Journal of Visualized Experiments
Publisher of new article	MyJove Corp.
Author of new article	Zoltan Cseresnyes
Expected publication date of new article	Sep 2018
Estimated size of new article (pages)	8
Requestor Location	Dr. Zoltan Cseresnyes Beutenbergstraße 11A Jena, 07745 Germany Attn: Dr. Zoltan Cseresnyes
Publisher Tax ID	EU826007151
Total	0.00 EUR
Terms and Conditions	

TERMS AND CONDITIONS

This copyrighted material is owned by or exclusively licensed to John Wiley & Sons, Inc. or one of its group companies (each a"Wiley Company") or handled on behalf of a society with

which a Wiley Company has exclusive publishing rights in relation to a particular work (collectively "WILEY"). By clicking "accept" in connection with completing this licensing transaction, you agree that the following terms and conditions apply to this transaction (along with the billing and payment terms and conditions established by the Copyright Clearance Center Inc., ("CCC's Billing and Payment terms and conditions"), at the time that you opened your RightsLink account (these are available at any time at http://myaccount.copyright.com).

Terms and Conditions

- The materials you have requested permission to reproduce or reuse (the "Wiley Materials") are protected by copyright.

- You are hereby granted a personal, non-exclusive, non-sub licensable (on a stand-alone basis), non-transferable, worldwide, limited license to reproduce the Wiley Materials for the purpose specified in the licensing process. This license, **and any CONTENT (PDF or image file) purchased as part of your order,** is for a one-time use only and limited to any maximum distribution number specified in the license. The first instance of republication or reuse granted by this license must be completed within two years of the date of the grant of this license (although copies prepared before the end date may be distributed thereafter). The Wiley Materials shall not be used in any other manner or for any other purpose, beyond what is granted in the license. Permission is granted subject to an appropriate acknowledgement given to the author, title of the material/book/journal and the publisher. You shall also duplicate the copyright notice that appears in the Wiley publication in your use of the Wiley Material. Permission is also granted on the understanding that nowhere in the text is a previously published source acknowledged for all or part of this Wiley Material. Any third party content is expressly excluded from this permission.

- With respect to the Wiley Materials, all rights are reserved. Except as expressly granted by the terms of the license, no part of the Wiley Materials may be copied, modified, adapted (except for minor reformatting required by the new Publication), translated, reproduced, transferred or distributed, in any form or by any means, and no derivative works may be made based on the Wiley Materials without the prior permission of the respective copyright owner.**For STM Signatory Publishers clearing permission under the terms of the STM Permissions Guidelines only, the terms of the license are extended to include subsequent editions and for editions in other languages, provided such editions are for the work as a whole in situ and does not involve the separate exploitation of the permitted figures or extracts,** You may not alter, remove or suppress in any manner any copyright, trademark or other notices displayed by the Wiley Materials. You may not license, rent, sell, loan, lease, pledge, offer as security, transfer or assign the Wiley Materials on a stand-alone basis, or any of the rights granted to you hereunder to any other person.

- The Wiley Materials and all of the intellectual property rights therein shall at all times remain the exclusive property of John Wiley & Sons Inc, the Wiley Companies, or their respective licensors, and your interest therein is only that of having possession of and the right to reproduce the Wiley Materials pursuant to Section 2 herein during the continuance of this Agreement. You agree that you own no right, title or interest in or to the Wiley Materials or any of the intellectual property rights therein. You shall have no rights hereunder other than the license as provided for above in Section 2. No right, license or interest to any trademark, trade name, service mark or other branding ("Marks") of WILEY or its licensors is granted hereunder, and you agree that you shall not assert any such right, license or interest with respect thereto

- NEITHER WILEY NOR ITS LICENSORS MAKES ANY WARRANTY OR REPRESENTATION OF ANY KIND TO YOU OR ANY THIRD PARTY, EXPRESS, IMPLIED OR STATUTORY, WITH RESPECT TO THE MATERIALS

OR THE ACCURACY OF ANY INFORMATION CONTAINED IN THE MATERIALS, INCLUDING, WITHOUT LIMITATION, ANY IMPLIED WARRANTY OF MERCHANTABILITY, ACCURACY, SATISFACTORY QUALITY, FITNESS FOR A PARTICULAR PURPOSE, USABILITY, INTEGRATION OR NON-INFRINGEMENT AND ALL SUCH WARRANTIES ARE HEREBY EXCLUDED BY WILEY AND ITS LICENSORS AND WAIVED BY YOU.

- WILEY shall have the right to terminate this Agreement immediately upon breach of this Agreement by you.

- You shall indemnify, defend and hold harmless WILEY, its Licensors and their respective directors, officers, agents and employees, from and against any actual or threatened claims, demands, causes of action or proceedings arising from any breach of this Agreement by you.

- IN NO EVENT SHALL WILEY OR ITS LICENSORS BE LIABLE TO YOU OR ANY OTHER PARTY OR ANY OTHER PERSON OR ENTITY FOR ANY SPECIAL, CONSEQUENTIAL, INCIDENTAL, INDIRECT, EXEMPLARY OR PUNITIVE DAMAGES, HOWEVER CAUSED, ARISING OUT OF OR IN CONNECTION WITH THE DOWNLOADING, PROVISIONING, VIEWING OR USE OF THE MATERIALS REGARDLESS OF THE FORM OF ACTION, WHETHER FOR BREACH OF CONTRACT, BREACH OF WARRANTY, TORT, NEGLIGENCE, INFRINGEMENT OR OTHERWISE (INCLUDING, WITHOUT LIMITATION, DAMAGES BASED ON LOSS OF PROFITS, DATA, FILES, USE, BUSINESS OPPORTUNITY OR CLAIMS OF THIRD PARTIES), AND WHETHER OR NOT THE PARTY HAS BEEN ADVISED OF THE POSSIBILITY OF SUCH DAMAGES. THIS LIMITATION SHALL APPLY NOTWITHSTANDING ANY FAILURE OF ESSENTIAL PURPOSE OF ANY LIMITED REMEDY PROVIDED HEREIN.

- Should any provision of this Agreement be held by a court of competent jurisdiction to be illegal, invalid, or unenforceable, that provision shall be deemed amended to achieve as nearly as possible the same economic effect as the original provision, and the legality, validity and enforceability of the remaining provisions of this Agreement shall not be affected or impaired thereby.

- The failure of either party to enforce any term or condition of this Agreement shall not constitute a waiver of either party's right to enforce each and every term and condition of this Agreement. No breach under this agreement shall be deemed waived or excused by either party unless such waiver or consent is in writing signed by the party granting such waiver or consent. The waiver by or consent of a party to a breach of any provision of this Agreement shall not operate or be construed as a waiver of or consent to any other or subsequent breach by such other party.

- This Agreement may not be assigned (including by operation of law or otherwise) by you without WILEY's prior written consent.

- Any fee required for this permission shall be non-refundable after thirty (30) days from receipt by the CCC.

- These terms and conditions together with CCC's Billing and Payment terms and conditions (which are incorporated herein) form the entire agreement between you and WILEY concerning this licensing transaction and (in the absence of fraud) supersedes all prior agreements and representations of the parties, oral or written. This Agreement may not be amended except in writing signed by both parties. This Agreement shall be binding upon and inure to the benefit of the parties' successors, legal representatives, and authorized assigns.

- In the event of any conflict between your obligations established by these terms and conditions and those established by CCC's Billing and Payment terms and conditions, these terms and conditions shall prevail.

- WILEY expressly reserves all rights not specifically granted in the combination of (i) the license details provided by you and accepted in the course of this licensing transaction, (ii) these terms and conditions and (iii) CCC's Billing and Payment terms and conditions.

- This Agreement will be void if the Type of Use, Format, Circulation, or Requestor Type was misrepresented during the licensing process.

- This Agreement shall be governed by and construed in accordance with the laws of the State of New York, USA, without regards to such state's conflict of law rules. Any legal action, suit or proceeding arising out of or relating to these Terms and Conditions or the breach thereof shall be instituted in a court of competent jurisdiction in New York County in the State of New York in the United States of America and each party hereby consents and submits to the personal jurisdiction of such court, waives any objection to venue in such court and consents to service of process by registered or certified mail, return receipt requested, at the last known address of such party.

WILEY OPEN ACCESS TERMS AND CONDITIONS

Wiley Publishes Open Access Articles in fully Open Access Journals and in Subscription journals offering Online Open. Although most of the fully Open Access journals publish open access articles under the terms of the Creative Commons Attribution (CC BY) License only, the subscription journals and a few of the Open Access Journals offer a choice of Creative Commons Licenses. The license type is clearly identified on the article.

The Creative Commons Attribution License

The Creative Commons Attribution License (CC-BY) allows users to copy, distribute and transmit an article, adapt the article and make commercial use of the article. The CC-BY license permits commercial and non-

Creative Commons Attribution Non-Commercial License

The Creative Commons Attribution Non-Commercial (CC-BY-NC)License permits use, distribution and reproduction in any medium, provided the original work is properly cited and is not used for commercial purposes.(see below)

Creative Commons Attribution-Non-Commercial-NoDerivs License

The Creative Commons Attribution Non-Commercial-NoDerivs License (CC-BY-NC-ND) permits use, distribution and reproduction in any medium, provided the original work is properly cited, is not used for commercial purposes and no modifications or adaptations are made. (see below)

Use by commercial "for-profit" organizations

Use of Wiley Open Access articles for commercial, promotional, or marketing purposes requires further explicit permission from Wiley and will be subject to a fee.
Further details can be found on Wiley Online Library
http://olabout.wiley.com/WileyCDA/Section/id-410895.html

Other Terms and Conditions:

v1.10 Last updated September 2015

Questions? customercare@copyright.com or +1-855-239-3415 (toll free in the US) or +1-978-646-2777.

GUI_Autorotate Python file

Click here to access/download
Supplemental Coding Files
GUI_Autorotate.py

AutoRotate_v2.0 Blender file

Click here to access/download

Supplemental Coding Files

AutoRotate_v2.0.blend

Trains_SOM_v1_0

Click here to access/download
Supplemental Coding Files
Trains_SOM_v1_0.m